Radiation-induced and chemical formation of gold clusters

Elisabeth Gachard, Hynd Remita, Jamal Khatouri, Bineta Keita, Louis Nadjo and Jacqueline Belloni*

Laboratoire de Physico-Chimie des Rayonnements, (CNRS URA 75), Université Paris-Sud, 91405 Orsay, France

The kinetics of the γ-radiolytical or chemical reduction of $Au^{III}Cl_4^-$, or of the combination of both methods, is followed as a function of the experimental conditions through the time evolution of the surface plasmon spectrum of the gold nanoparticles formed or of their sizes as observed by AFM imaging. It appears from the discussion on the mechanism that even with the strongly reducing radiolytic radicals, the low valency Au^I ions are somewhat protected by the more concentrated Au^{III} ions from reduction, up to a ratio of $Au^I/Au^{III} = 1$, and are stabilized for hours, unless clusters or 2-propanol (or PVA, but more slowly) catalyze their disproportionation. The cluster concentration increases correlatively with the dose.

2-Propanol or PVA are mild reducing agents and are unable to reduce Au^{III} directly except at the surface of clusters, previously formed, for instance, by partial radiolytic reduction. In this case, the cluster concentration remains the same but the size obtained after reduction by the alcohol increases slowly with time up to 100–500 nm, as in a development process. In order to avoid the relative extent of this development, associated with chemical reduction and even with the direct γ-reduction of Au^{III}, in particular the Au^I disproportionation and reduction steps, high dose rate radiolysis has been used up to total reduction of the same solutions. The mechanism of reduction and growth, step-by-step, is discussed.

Clusters are known to exhibit a very specific reactivity, which depends on their nuclearity.[1] Their catalytic efficiency is also controlled by their size. However, one of the most important reactions concerned by metal cluster reactivity is precisely the nucleation and growth of clusters, for instance when generated by the reduction of ionic precursors.[2–5] It seems that most of the features presented by the final clusters depend on the synthesis conditions under which clusters formed during the early steps of the reduction are active in further growth. The elementary steps of the reduction of lower valency ions to atoms and clusters are known from pulse techniques, generally pulse radiolysis by electron accelerator.[6,7]

The aim of this work is to compare different ways to synthesize metal clusters in solution: by radiolysis in both regimes (γ-radiolysis and electron pulse irradiation), by electron UV photodetachment and by chemical reduction of aqueous solutions of ionic precursors. Gold clusters are easily observed by their surface plasmon spectrum around 520 nm. We investigated, by optical spectroscopy and by AFM (atomic force microscopy) imaging, the effect of the γ-irradiation dose and the influence of other solutes on the reduction of trivalent gold ions, the formation rate of the successive valencies up to the zerovalent state and the nucleation rate of small clusters. The results are compared with the growth of gold clusters formed by mild reducing molecules in order to study the catalytic influence of small clusters acting as reduction nuclei. The kinetics of the chemical reduction of trivalent gold ions by methanol[8] and polyalcohols[9] have been already studied. Detailed investigations of the reduction by pulse radiolysis of metal ions and of metal cluster growth have been published,[2,4–7,10,11] namely in the case of monovalent gold cyanide.[12]

Experimental

The chemicals used are pure grade reagents. The gold salt is $KAuCl_4$ (Degussa). The reduction is achieved in aqueous solution with added 2-propanol (Prolabo) as an $OH^{\cdot}$ and $H^{\cdot}$ scavenger and polyvinyl alcohol (PVA, MW 86000, 98% hydrolyzed, Aldrich) as a surfactant. Solutions were thoroughly deaerated by flushing N_2 gas. The γ-irradiation source of the laboratory is a ^{60}Co γ-facility of 7000 Ci with a maximum dose rate of 10 kGy h^{-1}. The electron irradiation is performed with a 20 kW and 10 MeV electron accelerator (CARIC Society) delivering trains of 14 ms (10–350 Hz) pulses with a mean dose rate of 2.2 kGy s^{-1} (or 7.9 MGy h^{-1}). The solutions were stored in the dark as soon as prepared and also once irradiated. A new sample is used for each irradiation dose. Then the kinetics after irradiation are followed on the same sample with increasing time. The surface plasmon spectra of gold clusters produced by the reduction were recorded in suprasil optical cells with a Hewlett Packard 8453 spectrophotometer. Some experiments have been carried out by UV excitation (Hg light).

For AFM imaging, one drop of the solution is deposited on a HOPG (highly oriented pyrolytic graphite) support and dried under N_2 gas, also used to spread out the film as uniformly as possible. This technique gives reproducible images from sample to sample prepared under the same conditions. Therefore, the images can be considered as reflecting reliably the relative density of the sol particles. A Nanoscope (III) (Digital Instruments, Santa Barbara, CA) equipped with an Extender Electronics Module was used. The images were acquired in tapping mode, using a silicon cantilever. None of the images has been filtered.

Results

The solutions are quite stable before irradiation. No band is detected except that of $Au^{III}Cl_4^-$ around 200–300 nm. Because the kinetics of thermal reactions after the end of the γ-irradiation are slow, in the range of hundreds of min, the processes occurring during the irradiation may be separately observed provided the dose is absorbed within a few min and the spectrum is recorded immediately after the end of the irradiation. Most of the experiments have been achieved at a dose rate of 10 kGy h^{-1}. The spectra are recorded under nitrogen atmosphere. However, they do not change when the sample is exposed to air.

Au^{III} reduction by γ-irradiation

A typical spectrum of a colloidal solution of gold just after the end of the γ-irradiation (less than 5 min) of a 10^{-3} mol l^{-1} auric solution in the presence of 0.1 mol l^{-1} PVA and/or 0.2 mol l^{-1} 2-propanol is shown in Fig. 1. It corresponds to the surface plasmon spectrum of gold nanoparticles with a band maximum at 520 nm.

The spectrum shape in the 400–700 nm range does not change from the lowest doses up to total reduction. When increasing the dose, the maximum intensity of the surface plasmon band increases up to a limiting value corresponding to the total reduction of the solution (Fig. 2). The results depend drastically on the solutes added to the auric solutions. In the presence of PVA, the absorbance at the plateau is quite stable. In the presence of only 2-propanol, the plateau of the absorbance and the initial increase are about 50% higher and the band is narrower than with PVA. At doses larger than 10 kGy the clusters that are not stabilized flocculate partly, and the absorbance no longer represents the total metal concentration. The position of the maximum with 2-propanol is slightly shifted to 530 nm, relative to 520 nm with PVA. Also, the red part of the spectrum with 2-propanol is in fact more intense than with PVA, a signature of larger particles. However, in the presence of both PVA and 2-propanol, the curve is close to the curve at the same initial auric ion concentration with PVA only. Assuming that the plateau corresponds to a total reduction, we find that the extinction coefficient per atom is $\varepsilon(Au)_{n,\,PVA} = 3.2 \times 10^3$ l mol^{-1} cm^{-1} (in agreement with a previous determination[13]) and $\varepsilon(Au)_{n,\,i\text{-PrOH}} = 4.7 \times 10^3$ l mol^{-1} cm^{-1} when only 2-propanol is added.

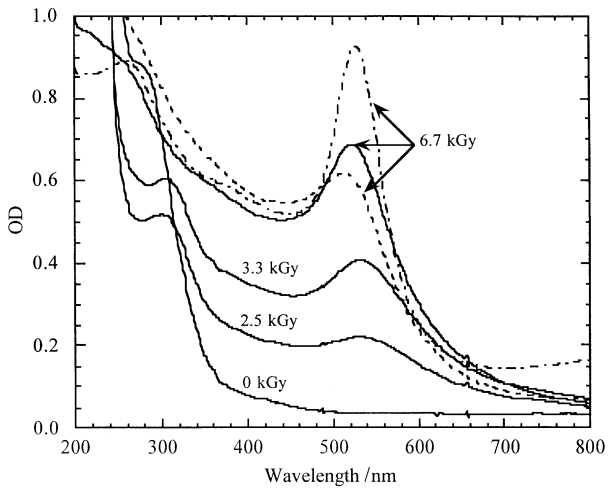

Fig. 1 Evolution of the optical absorption spectrum with dose in γ-irradiated 10^{-3} mol l^{-1} auric ($KAuCl_4$) solutions. Doses are indicated on the spectra. Optical path: 2 mm. (———) 0.1 mol l^{-1} PVA, 0.2 mol l^{-1} 2-propanol; (– – – –) 0.1 mol l^{-1} PVA; (–·–·–·) 0.2 mol l^{-1} 2-propanol

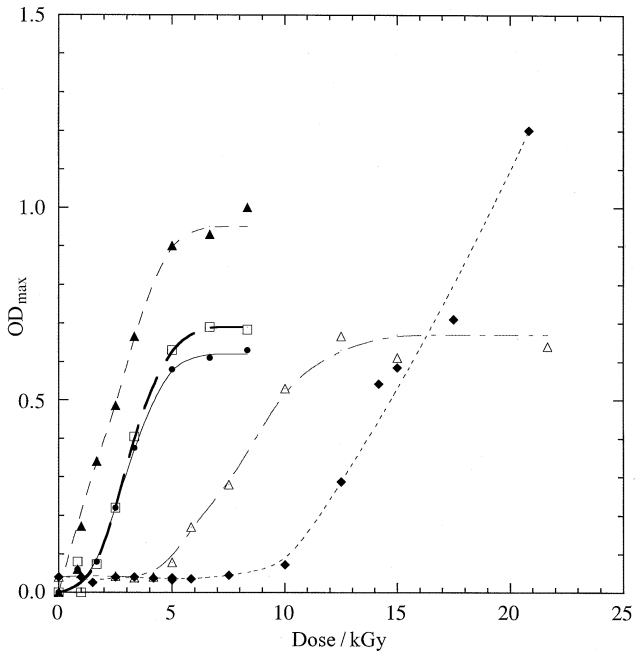

Fig. 2 Evolution of the absorbance at the wavelength maximum (λ_{max} = 520 nm) *vs.* dose at the end of the irradiation. Optical path: 2 mm. Dose rate: 10 kGy h^{-1}. (△) 10^{-3} mol l^{-1} $KAuCl_4$; (◆) 2×10^{-3} mol l^{-1} $KAuCl_4$; (●) 10^{-3} mol l^{-1} $KAuCl_4$, 0.1 mol l^{-1} PVA; (▲) 10^{-3} mol l^{-1} $KAuCl_4$, 0.2 mol l^{-1} 2-propanol (λ_{max} = 530 nm); (□) 10^{-3} mol l^{-1} $KAuCl_4$, 0.1 mol l^{-1} PVA, 0.2 mol l^{-1} 2-propanol

An important feature of the curves of Fig. 2 is the absorbance variation at low dose. In the presence of 2-propanol only, the increase is linear up to the almost complete reduction at 5 kGy. In contrast, the absorbance in other solutions, without additives or with PVA, does not increase linearly but starts to increase after a short induction dose (<1 kGy for PVA with or without 2-propanol). The phenomenon is much more pronounced when neither surfactant nor 2-propanol is added to the 10^{-3} or 2×10^{-3} mol l^{-1} auric solutions. The induction doses are about 5 and 10 kGy, respectively (Fig. 2). However, the extinction coefficient is the same as with PVA. At 2×10^{-3} mol l^{-1}, the plateau expected at about OD = 1.3 was not reached due to flocculation. It is obvious from the curves of Fig. 2 that at any dose the radiolytic yield is much lower in the absence of an alcohol (2-propanol or PVA) than in its presence.

The primary species generated by the radiation interaction with the solvent water are:

$$H_2O \rightarrow e_{aq}^-,\ H_3O^+,\ H^{\cdot},\ H_2,\ OH^{\cdot},\ H_2O_2 \qquad (1)$$

At pH 7 the radiolytic yields of the radicals are: $G(e_{aq}^-) = 2.7$, $G(H^{\cdot}) = 0.55$, $G(OH^{\cdot}) = 2.8$ elementary species per 100 eV absorbed ($G = 1$ corresponds to 9×10^{-5} mol l^{-1} per kGy).

Note that e_{aq}^- may be formed also by photodetachment from anions in solution when exposed to UV light:

$$Cl^- \rightarrow Cl^{\cdot} + e_{aq}^- \qquad (2)$$

For this reason, the solutions were stored in the dark before and after γ-irradiation. Gold ions $Au^{III}Cl_4^-$ are reduced by e_{aq}^- [$E^\circ(H_2O/e_{aq}^-) = -2.87$ V_{NHE} [14,15]] into Au^{II}, as already shown by pulse radiolysis studies:[16]

$$Au^{III}Cl_4^- + e_{aq}^- \rightarrow Au^{II}Cl_4^{2-} \qquad (3)$$

In certain experiments, we added 2-propanol in order to scavenge $OH^{\cdot}$ radicals whose powerful oxidizing properties would otherwise cause a reverse oxidation of the gold atoms and low-valency ions formed by the solvated electrons, as shown by the lower yields found in the absence of alcohols (Fig. 2). The $H^{\cdot}$ atoms are scavenged by the alcohol as well:

$$(CH_3)_2CHOH + OH^{\cdot}\ (H^{\cdot}) \rightarrow (CH_3)_2\dot{C}OH + H_2O\ (H_2) \qquad (4)$$

The $(CH_3)_2\dot{C}OH$ alcohol radicals exhibit reducing properties {$E^\circ([(CH_3)_2CO + H^+]/(CH_3)_2\dot{C}OH) = -1.8$ V_{NHE} at pH 7}[17] and they contribute to the reduction yield of gold ions:

$$Au^{III}Cl_4^- + (CH_3)_2\dot{C}OH \rightarrow Au^{II}Cl_4^{2-} + (CH_3)_2CO + H^+ \qquad (5)$$

The following step is the disproportionation of Au^{II} [$k_6 = (0.48 \pm 0.12) \times 10^9$ l mol^{-1} s^{-1}]:[16]

$$2\ Au^{II}Cl_4^{2-} \rightarrow Au^{III}Cl_4^- + Au^{I}Cl_2^- + 2\ Cl^- \qquad (6)$$

When Au^{III} ions are partly depleted after a certain dose by reactions (3) [and (5) if an alcohol is present], then accumulating aurous ions Au^{I} may also compete for the scavenging of

e_{aq}^- [and $(CH_3)_2\dot{C}OH$], so that they are reduced during the latter part of the irradiation into Au^0 atoms, which are precursors of clusters:

$$Au^{I}Cl_2^- + e_{aq}^- \text{ [or } (CH_3)_2\dot{C}OH] \rightarrow Au^0Cl_2^{2-} \text{ [or } + (CH_3)_2CO + H^+] \quad (7)$$

It is remarkable that the induction dose assigned to the start of Au^I reduction is doubled when the initial $Au^{III}Cl_4^-$ concentration is doubled, which confirms the competition between reactions (3) [and (5)] and (7). The thermodynamics of this reaction force us to consider the single atom as being complexed. The monovalent gold ions $Au^{I}Cl_2^-$ are known from electrochemistry to disproportionate in the presence of electrodes. If they are not reduced by the radiolytic species, they are supposed to disproportionate to give Au^{II} and zerovalent gold,[18] but this does not occur if they are formed as isolated atoms [reaction (7)] since a catalyst is required (see discussion).

By analogy with the reduction mechanism of monovalent silver ions[1,2,6] and other ions,[10] the radiolytic formation of gold atoms is probably followed by association of atoms with an excess of ions [reactions (8)], dimerization [reaction (9)] and finally by aggregation of these species into clusters of higher nuclearity surrounded by chloride anions [reaction (10)]:

$$Au^0Cl_2^{2-} + Au^{I}Cl_2^- \rightarrow (Au_2^+)_{Cl^-} \quad (8)$$

$$2(Au_2^+)_{Cl^-} \rightarrow (Au_4^{2+})_{Cl^-} \quad (9)$$

$$(Au_q^{z+})_{Cl^-} + (Au_p^{y+})_{Cl^-} \rightarrow (Au_n^{x+})_{Cl^-} \quad (10)$$

At any stage of the coalescence, the ions adsorbed on the clusters may be reduced as well by the radiolytic species. The role of added PVA in the system is twofold. Due to its residual carboxylate groups the surfactant PVA interacts with the metal atoms of the cluster surface and stabilizes the clusters by inhibiting their coalescence.[19] But the polyalcoholic character of PVA may also contribute, mostly in the absence of 2-propanol, to the scavenging of $H^\cdot$ and $OH^\cdot$ [similar to reaction (4)]. The PVA radical thus formed contributes to the reduction of gold ions, as shown by the similarity between the curves in Fig. 2 with PVA alone or associated with 2-propanol.

When the spectrum intensity is plotted *vs.* the dose absorbed (Fig. 2), for example at the band maximum (λ_{max} = 530 nm), a linear relation is observed in the presence of 2-propanol only. From the extinction coefficient $\varepsilon(Au)_{n,\,i\text{-PrOH}}$, we determine a radiolytic yield of $G(Au^0) = 2$, which corresponds to a total reduction yield $G(\text{red}) = 3 \times G(Au^0) = 6$, according to the above mechanism [reactions (1)–(10)].

It is remarkable that in PVA solutions (Fig. 2) the yield at low dose is almost zero during an induction period (of 1 to 1.5 kGy depending on the conditions). However, the amount of clusters formed at about 5 kGy, which is close to the plateau in the presence of PVA (with or without 2-propanol), corresponds again to a mean yield of $G(Au^0) = 2 = G(\text{red})/3$. In the absence of alcohols, $OH^\cdot$ radicals are not scavenged and the reduction yield must be lower, as observed in Fig. 2 where a mean value of $G(Au^0) = 1$ only is observed after 10 kGy for $[Au^{III}] = 10^{-3}$ mol l^{-1} and even after 20 kGy for $[Au^{III}] = 2 \times 10^{-3}$ mol l^{-1}. Correlatively, the absorbance in the UV region at 293 nm (where the auric ions absorb and the extinction coefficient does not depend on the Cl^- or Au^{III} concentrations), decays linearly with increasing dose, at least up to 5 kGy. However, Au^I is certainly formed by reaction (6) after Au^{III} reduction and its absorption contribution in the same region is negligible.[20]

Comparison of the results on Au^{III} disappearance and Au_n formation *vs.* dose up to 5 or 10 kGy within the induction region raises the serious question of the material balance. Actually, it is clear that the reduced auric ions are not in the form of atoms belonging to clusters whose concentration would be measured by the specific surface plasmon spectrum. However, such a spectrum in a partially reduced solution with 1.5 kGy (in the absence of other additives, therefore of any reducing agent) develops slowly with time (Fig. 3), and after 5 h corresponds to a yield of $G(Au^0)_n = 1$, as if some metastable precursors have been transformed into clusters.

Different assumptions may be made about the gold species distinct from Au^{III} or Au_n, which are missing in the material balance at the end of the irradiation.

Before the formation of aggregates, small zerovalent gold oligomers may be formed. They are known to exhibit a spectrum less intense than clusters do and their absorbance increases to the blue without any maximum, at least in the visible.[12] However, if they were present at low dose and at the end of irradiation, an absorbance would be observed because the extinction coefficient in the near UV is rather high. Moreover, no supplementary absorbance is detected if a salt such as sodium perchlorate (10^{-2} mol l^{-1}) is added after the 1.0 kGy irradiation, in order to increase the ionic strength of the solution and to help the possible oligomers flocculate into clusters. We conclude that the balance of Au^{III} reduction is not completed by small zerovalent oligomers.

In contrast, if to the same 1.5 kGy irradiated solution are added gold clusters (10^{-3} mol l^{-1}), prepared in advance by irradiation at total reduction (10 kGy) of another sample, the intensity of the specific spectrum of preformed gold clusters immediately increases as if the addition of nuclei (without reducing properties *per se*) had transformed ions of a valency lower than III into supplementary zerovalent gold, which would correspond to a cluster yield of 1 or $G(\text{red}) = 3$. Moreover, when irradiated in the presence of preformed clusters, the auric solution is reduced into Au_n from the lowest doses with a yield of $G(\text{red}) = 3$ and no induction time is observed, in contrast with the results of Fig. 2. Since Au^{II} ions disproportionate too fast to be metastable [reaction (6)], the simplest explanation is to invoke the presence of Au^I species that could be stabilized (even in the presence of air) as long as clusters are not yet formed or added. The Au^I concentration represents the number of equivalents of reduced Au^{III} because no other stable valency is formed at low dose. Therefore, we conclude that the post-irradiation increase of the 520 nm absorbance is due to a very slow disproportionation of Au^I, after adsorption onto native or added clusters:

$$2\ Au^I, Au_n \rightarrow (Au^{II}, Au_n)_{Cl^-} + Au_{n+1} \quad (11)$$

This reaction is followed by Au^{II} disproportionation [reaction (6)]. The point of Au^I metastability and very slow disproportionation in the absence of clusters will be discussed in the

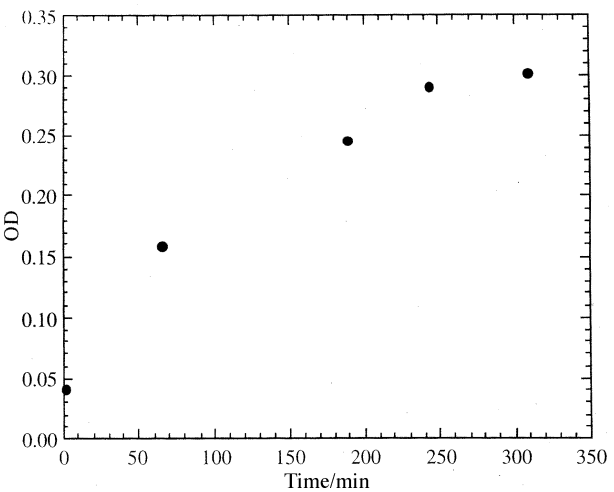

Fig. 3 Time evolution of the absorbance at 520 nm after the end of γ-irradiation with a dose of 1.5 kGy in a 10^{-3} mol l^{-1} $KAuCl_4$ solution. Zero time is the start of irradiation. Optical path: 10 mm

last section. Recently, a similar process of catalyzed disproportionation of Au^{I} has been evidenced on Au foils or on early-formed clusters.[21] The length of the induction times in the chemical reduction kinetics of Au^{III} by basic methanol or by polyalcohols have been found to depend on the presence of metal clusters or other colloidal particles.

During the induction period, the reduction yield of Au^{III} into Au^{I} would be, according to this assumption: $G(Au^{I}) = G(-Au^{III}) = \frac{3}{2}G(Au^{0})_n = 3$ or 1.5 equiv. per 100 eV, with or without alcohols, respectively. Under similar conditions in the presence of methanol, previous authors found a disappearance yield $G(-Au^{III}) = 3$ [18] and 0.7 ions per 100 eV in aerated solutions.[22] Note that the transitory stabilization of unusual low valency transition metal ions has been already found in the case of other systems such as iridium,[23] platinum,[24] palladium,[25] copper[26,27] and nickel[28] for at least up to 200 ms. Competition between Au^{III} [reactions (3) and (5)] and Au^{I} [reaction (7)] for the scavenging of e_{aq}^{-} and reducing radicals depends on the ratio $[Au^{III}]/[Au^{I}]$. When the initial concentration of Au^{III} increases, the reduction of Au^{I} requires a larger accumulation of Au^{I} before being efficient and the induction time is longer (Fig. 2). When the induction time ends (at 5 kGy for 10^{-3} mol l^{-1} or at 10 kGy for 2×10^{-3} mol l^{-1}), the ratio is 1 and the fraction of Au^{III} reduced is 50%, which means that the rate constants k_2, k_4 and k_6 are of the same order of magnitude. As soon as the Au^{I} reduction begins, the atoms formed coalesce into clusters and, as we have observed when clusters are added, the clusters catalyze the disproportionation of Au^{I}, thus further increasing cluster growth. Thus, the product of Au^{III} reduction is no longer Au^{I} but Au_n^{0}. After the disproportionations of reactions (11) and (6), $G(-Au^{III})_{10kGy} = G(Au_n^{0})_{10kGy} = 1.0$ because Au^{III} is now in part reversibly formed.

The temporary stabilization of Au^{I} will later cause a catalytic disproportionation restricted first to the cell walls (and dusts) and then to the surface of clusters produced early-on in the bulk.[8] This process will contribute to the growth of clusters. In order to reduce Au^{I} into Au^{0} earlier than this possible disproportionation, irradiation experiments have been carried out through a high dose rate source (electron accelerator). The reduction by e_{aq}^{-} and $(CH_3)_2\dot{C}OH$ is thus achieved within ≈ 1 s. Thus, the Au^{I} ions are directly reduced into isolated Au^{0}, which then coalesce. The surface plasmon spectrum of this sample is somewhat different from previous ones. The maximum is shifted to 512 nm and $\varepsilon = 2.6 \times 10^{3}$ l mol^{-1} cm^{-1}.

Similar phenomena concerning the induction time before cluster formation, as observed after γ-irradiation, have also been found when a partial reduction is initiated by electrons generated through UV exposure with a Hg lamp [reaction (2)].

The set of images in Fig. 4, presents observations by AFM of samples dried immediately after the end of γ-irradiation at various doses: (*i*) at 1.5 kGy just at the beginning of the cluster formation, (*ii*) then at 2 kGy during the formation, (*iii*) and finally at 5 kGy when the reduction is complete. The corresponding experiments were performed in the presence of 0.1 mol l^{-1} PVA and 0.2 mol l^{-1} 2-propanol. It is noteworthy that the images are particularly uniform in aspect throughout the sample surface. This observation induces us to show relatively large scale images. However, size determinations were performed on smaller scale images. It must also be pointed out that, as expected,[29] the phase mode display shows sharper contours than the height mode images. However, the two modes are presented simultaneously for all images. In the micrograph of Fig. 4(*A*), the size of the scarce clusters present is not larger than 5 nm ($n = 155$ atoms). At 2 kGy the density of clusters is much higher and the sizes of the majority of them are rather monodisperse around the value of 5 nm, even though a few larger clusters appear [Fig. 4(*B*)]. At complete

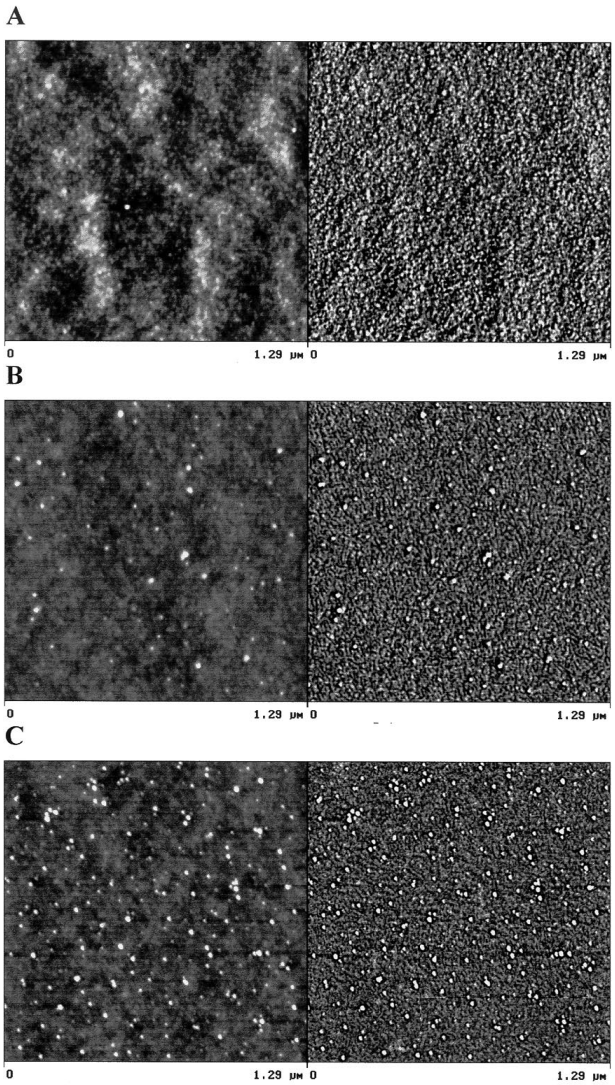

Fig. 4 AFM images showing the effect of γ-irradiation dose on the cluster concentration. Each solution contains 10^{-3} mol l^{-1} Au^{III}, 0.1 mol l^{-1} PVA and 0.2 mol l^{-1} 2-propanol (see Fig. 2 and text for further details). Left: height mode (*z* range 25.0 nm). Right: phase mode (*z* range 18.0°). (*A*) 1.5 kGy (9 min), (*B*) 2 kGy (12 min), (*C*) 5 kGy (30 min)

reduction, the size of the largest clusters is still the same but the density is now markedly increased [Fig. 4(*C*)]. The results suggest that, after the first step, when zerovalent gold is not yet much formed because Au^{I} is stabilized, the newly created atoms contribute partly to letting the few small clusters already formed grow and partly to coalescing into new clusters with a rather reproducible stabilized upper size limit. Finally, the probability of the formation of new clusters predominates.

In a remarkable observation, AFM images reveal that the upper size limit of coalesced clusters, and hence the aggregation kinetics, depends strongly on the presence or absence of alcohol. For instance, in the absence of alcohol, with the other experimental conditions being exactly the same as for Fig. 4(*A*), the large clusters are much more abundant, with an average size of 20 to 50 nm. (This results appears consistent with the creation of fewer nuclei in the absence of alcohol.)

Time evolution of the spectrum after the end of γ-irradiation (partial reduction)

As shown in Fig. 5–7, when a 10^{-3} mol l^{-1} auric solution containing PVA (with or without 2-propanol) is only partially reduced (dose = 1.5 kGy) and the evolution of the spectrum is recorded again at different delay times after the end of the

irradiation, we observe a supplementary post-irradiation increase of the spectrum intensity (with no change in shape), which corresponds to the surface plasmon band of gold clusters. The spectrum develops eventually at quite long time (a few weeks) to the total reduction of $Au^{III}Cl_4^-$ ions [as seen for 10^4 min in Fig. 5(*c*)], at least for the higher concentrations; and therefore, at a much higher yield than the total radiolytic reduction $G(\text{red}) = 6$. This increase is much higher than in the absence of alcohols, where it corresponded just to the disproportionation of metastable Au^I [reaction (11)]. The absorbance in the visible region of an unirradiated solution is negligible even after hours [Fig. 6(*a*)]. Therefore, the slow gold ion reduction is due to a spontaneous chemical process indirectly initiated by the irradiation. The slow post-effect observed cannot be assigned, of course, to surviving primary radicals because their lifetime is too short.

The influence of the PVA concentration in the absence of 2-propanol is shown in Fig. 5. The kinetics are divided into two distinct components. The first one (I) lasts for about 50 min, and the absorbance increase is somewhat faster than for the second component II. At the end of component I, the quantity of gold atoms corresponds to a reduction yield of $G(Au^0) = G(\text{red})/3 = 2$. The larger the 520 nm absorbance just after the end of irradiation, the faster is its further post-irradiation increase. The rate depends on the PVA concentration, mostly above 0.1 mol l^{-1}. The rate of II, much slower, increases also with the PVA concentration (Fig. 5).

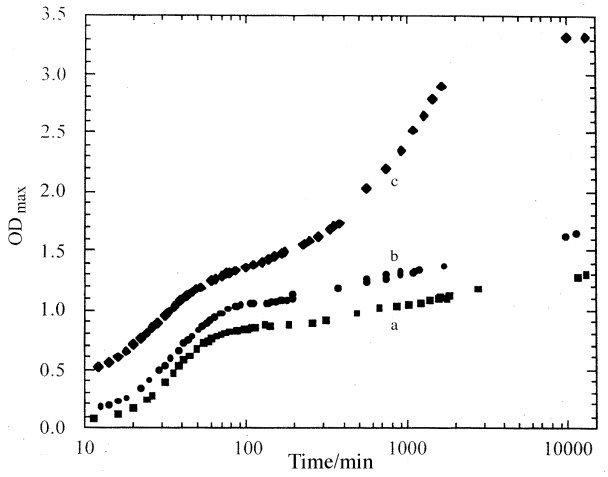

Fig. 5 Time evolution of the absorbance at 520 nm, after the end of γ-irradiation at a dose of 1.5 kGy, in a 10^{-3} mol l^{-1} auric ($KAuCl_4$) solution with various PVA concentrations: (*a*) 0.05, (*b*) 0.1, (*c*) 0.2 mol l^{-1}. Optical path: 10 mm. Components I and II are presented on the same log scale

Another set of experiments was made in the presence of 2-propanol without PVA (Fig. 7). In this case the absorbance at the end of irradiation is much higher than with PVA and already corresponds to a yield of total radical scavenging $G(\text{red}) = 6$. Clearly, Au^I is not stabilized and is already disproportionated into Au^0 so that component I is over within the irradiation time. However, a post-effect with a supplementary absorbance increase in II is observed. It is apparently of small amplitude because the spectrum changes announce a flocculation or at least the growth of the clusters, which are no longer stabilized by a surfactant.

As different species may be involved in the chemical post-irradiation reactions, we studied first the effect on the kinetics of the addition of preformed clusters in an unirradiated Au^{III} solution [Fig. 6(*c*)]. It is seen that the reduction occurs indeed with a rate comparable to the post-effect II observed after irradiation, as if a reduction by alcohols initiated by the added clusters acting as catalytic germs would suffice to account for the slow increase of the second component. We propose a chemical reaction restricted exclusively to the surface of the formerly produced clusters:

$$Au^{III}, Au_n + ROH \rightarrow Au^{II}, Au_n + H^+ + RO^{\cdot} \qquad (12)$$

followed by reactions (6), (7) and (11). The new atoms formed in reaction (11) increase the nuclearity of the cluster as in a catalytic development process.[30] Likewise, 2-propanol in basic medium has been found to reduce Ag^+ at the surface of $(Ag_2O)_n$ particles.[31]

AFM images, scanned on samples deposited at various times after the end of the irradiation process, confirm the important variations in aggregation up to crystallization kinetics in the presence or absence of alcohol. A sample irradiated with 1.5 kGy in the absence of alcohol, was deposited for observation 30 days after the irradiation. It is illustrated in Fig. 8(*A*) and (*B*), which shows the height mode image (*A*) and the corresponding phase image (*B*). Large crystallites are observed. Incidentally, we note that the contours of the crystallites are sharper on the phase image as expected.[29] Fig. 8(*C*) and (*D*) is obtained by zooming in a representative area of Fig. 8(*A*) and (*B*) and rescanning directly. It provides a sharper view on the morphology of the crystallites. They appear mostly as large, regularly shaped crystallites of apparent surface area ranging roughly from 25 × 50 to 140 × 190 nm^2. Their morphology would suggest crystallization in a simple

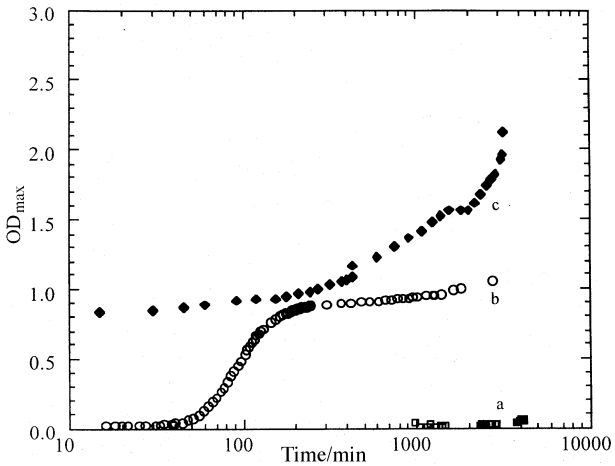

Fig. 6 Time evolution at room temperature of the absorbance at 520 nm in a 10^{-3} mol l^{-1} $KAuCl_4$ solution with 0.2 mol l^{-1} 2-propanol and 0.1 mol l^{-1} PVA: (*a*) non-irradiated solution, (*b*) after the end of irradiation at a dose of 1 kGy, (*c*) non-irradiated solution after addition of preformed germs

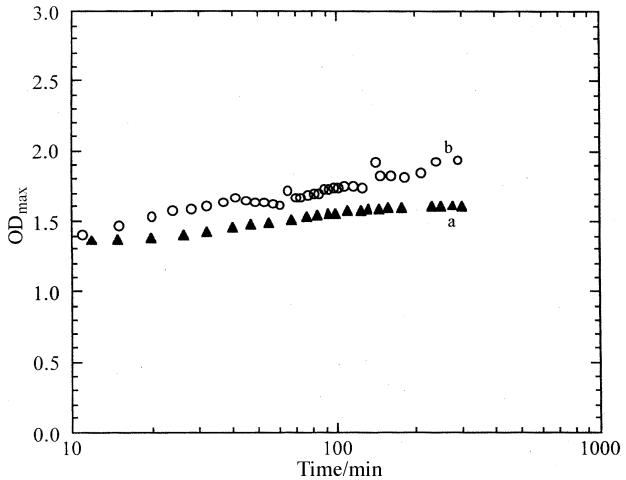

Fig. 7 Time evolution of the absorbance at 520 nm, after the end of irradiation, in an auric solution (10^{-3} mol l^{-1} $KAuCl_4$) with various 2-propanol concentrations: (*a*) 0.02, (*b*) 0.1 mol l^{-1}. Initial dose = 1.5 kGy. Optical path: 10 mm

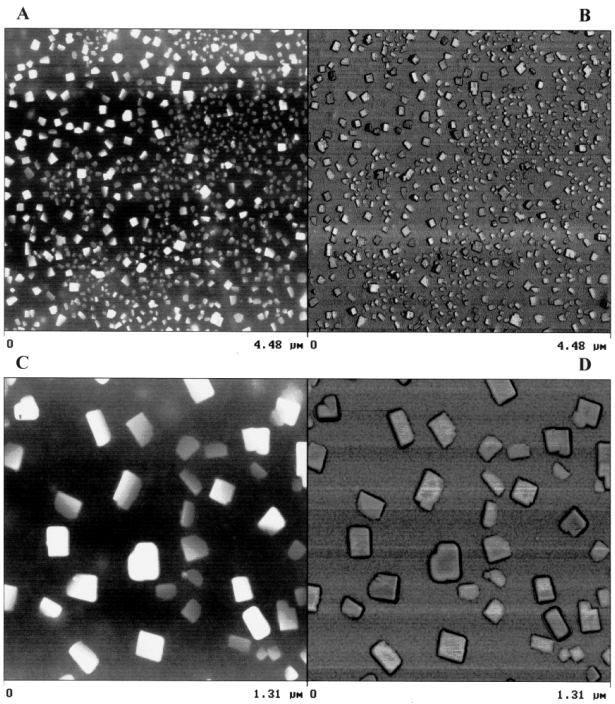

Fig. 8 Tapping mode AFM images of the species formed in a solution irradiated with γ rays (1.5 kGy), then deposited on HOPG 30 days after the irradiation and dried under a mild N_2 stream for visualization. The solution contains 10^{-3} mol l^{-1} Au^{III} and PVA but *no alcohol* (see Fig. 2). (*A*) Height mode (*z* range 80.0 nm) image and (*B*) phase (*z* range 42.2°) image, run simultaneously on the same area of the sample. (*C*) and (*D*) Close-up images showing the same area as in (A) and (B), respectively

classical system, maybe owing to the specific process of particle formation by development[30] [reaction (12)] under our experimental conditions. However, further studies, both with AFM and various diffraction techniques, will allow complete characterization of the corresponding crystallographic system. The same sample, irradiated with 1.5 kGy in the presence of alcohol [thus corresponding to Fig. 4(*A*) for the dose] and deposited for imaging six weeks later, also shows large crystallites. Roughly the same shapes are obtained in the presence and absence of alcohol. Here, it can be assumed that total reduction is finally achieved after this duration. Then, even with this assumption, it is observed that the number of crystallites is rather comparable to that at low dose [Fig. 4(*A*)], except that the sizes are much larger. Note that, for the same total amount of reduced atoms, the cluster concentration is a linear function of $(n)^{-3}$ and, thus, the concentration of 100 nm clusters must be much less than that of nanometric ones. A striking difference is revealed here between the effect of γ-radiolysis alone or in combination with further chemical reduction. The chemical reduction, which takes place after the irradiation, apparently does not create new clusters but contributes to letting the few pre-existing ones, induced during the 1.5 kGy irradiation, grow.

Another conclusion from the present AFM study is revealed by the examination at increasing time of the irradiated solutions: whether alcohol is present or not, the aggregation/crystallization process is quite slow and lasts for weeks.

In order to avoid completely the possible chemical growth by alcohols or by catalyzed disproportionation even during the irradiation time, some samples were also irradiated with a powerful and short pulse delivered by an electron accelerator that allowed ion reduction within a few seconds. A clear dose effect has been detected from AFM images. The experiments start from two identical solutions containing 10^{-3} mol l^{-1} Au^{III}, PVA and alcohol. After irradiation with 6.5 kGy and 4.5 kGy, respectively, the samples were deposited immediately on HOPG and dried under a stream of nitrogen for AFM observation. Fig. 9(*A*) and (*B*) shows the corresponding images. It must be emphasized that the images have been selected to represent as closely as possible the observations on the whole surface of the deposit on the HOPG support. Fig. 9(*A*) pertains to the 6.5 kGy irradiation and corresponds to complete reduction. It shows a large number of clusters, which are rather small and uniform in size and distribution. The sample deposited 4 h after the end of the irradiation shows the same aspect. From this observation, it must be concluded that little, if any, evolution of the cluster sizes has occurred and no development may be observed. Fig. 9(*B*) corresponds to 4.5 kGy. The contrast with Fig. 9(*A*) is striking. A few but significant number of large clusters have already appeared at the end of the irradiation. Here again, the sample deposited after 4 h was also examined and revealed fewer, but larger clusters compared to those of Fig. 9(*B*). Clearly, the sample with 4.5 kGy irradiation is different from that with 6.5 kGy, and also shows some evolution, which is not seen with the sample of Fig. 9(*A*). All these observations support completely the experiments by spectroscopic techniques and fit in with our assumptions and reasoning that will be developed in more detail in the following.

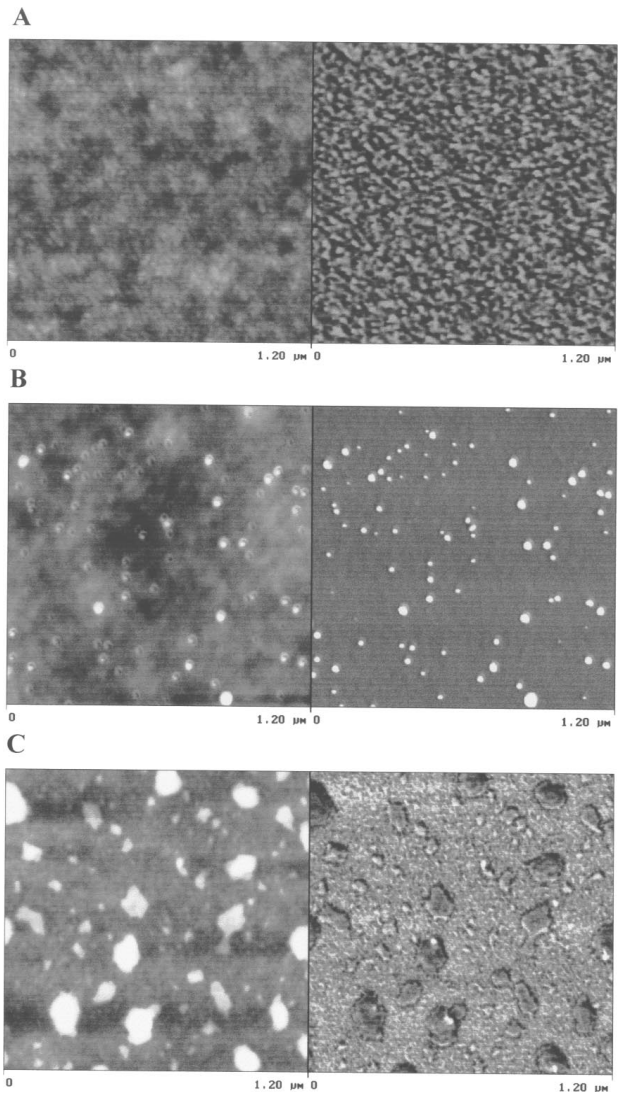

Fig. 9 Dose and temperature effects observed by tapping mode AFM on samples deposited from solutions irradiated with the CARIC set-up. Each solution contains 10^{-3} mol l^{-1} Au^{III}, PVA and alcohol (see Fig. 2; for further details, see text). Each sample was deposited on HOPG and dried immediately after the irradiation. Left: height mode [*z* range 7.00 nm for (*A*), (*B*); 25.0 nm for (*C*)]. Right: phase mode (*z* range 20.0°). (*A*) 6.5 kGy, ≈20 °C; (*B*) 4.5 kGy, ≈20 °C; (*C*) 4.5 kGy, ≈30 °C

A complementary experiment with the CARIC apparatus deserves emphasis, because it shows the influence of temperature. Fig. 9(*C*) must be compared with Fig. 9(*B*) and illustrates the temperature effect. The samples have been irradiated with the same dose (4.5 kGy), at $T \approx 20\,^{\circ}C$ in Fig. 9(*B*) and at $T \approx 30\,^{\circ}C$ in Fig. 9(*C*), and the two samples were deposited immediately afterwards. Not unexpectedly, the kinetics of formation of very large clusters are favored by a rise in temperature.

Discussion

A general remark on the results obtained is that the features of the final clusters are strongly influenced in a precise way by the various conditions of the gold reduction, either *via* radiolysis (γ-rays or electrons) only or *via* chemical reduction, or both. The kinetics study emphasizes also the main factors that control the successive steps of the growth dynamics.

Au^{III} reduction

The slowest step II involves clusters, Au^{III} ions and alcoholic functions as the reducing agent. As similar kinetics were obtained even if the solution was not irradiated but exclusively in the presence of added clusters, we conclude that the slow reduction is initiated by the reduction of adsorbed Au^{III} on the clusters by an alcohol group (of 2-propanol or of PVA) [reaction (12)], followed by the successive disproportionations of Au^{II} [reaction (6)] and of Au^{I} adsorbed on clusters [reaction (11)]. This implies that the redox potential values of the couples are in the order:

$$E^{\circ}(Au^{III}/Au^{II}) < E^{\circ}[(CH_3)_2\dot{C}OH/(CH_3)_2CHOH] < E^{\circ}(Au^{III}, Au_n/Au^{II}, Au_n) \quad (13)$$

In contrast, the radiolytic reduction process is initiated by any encounter of free Au^{III} with solvated electrons or alcohol radicals [reactions (3) and (5)].

Au^{I} stabilization

Concerning the disproportionation of Au^{I}, the relative order of the potentials is

$$E^{\circ}(Au^{I}, Au_n/Au_{n+1}) > E^{\circ}(Au^{II}, Au_n/Au^{I}, Au_n) \quad (14)$$

to be compared with

$$E^{\circ}(Au^{I}/Au^{0}) < E^{\circ}(Au^{II}/Au^{I}) \quad (15)$$

The appearance of Au_n is therefore critical for the chemical reduction of Au^{III} by alcohols, which does not occur unless Au_n are already formed by radiolysis [Fig. 6(*a*)]. Similar observations were made for other metals, for example Cu,[26,27] which are stable in the valence I in the absence of metal clusters. Note that the disproportionation reaction (11) [with eqn. (14)] is quite similar, when $n \rightarrow \infty$, to the known Au^{I} disproportionation on a bulk electrode in the presence of Cl^-. However, when we compare the redox potential $E^{\circ}(Au^{I}/Au^{0})$ with the electrode potential $E^{\circ}(Au^{I}, Au_n/Au_{n+1})$, the difference may be indeed quite large because it includes the sublimation energy from the metal Au_n to isolated atoms Au^0. For the silver aquo system the potential of the single atom is -1.8 V_{NHE} [2] and for the cyano complex of Ag it is equal to -2.61 V_{NHE}.[32] The potential of the couple Cu^{I}/Cu^{0} (isolated copper atoms) was estimated to be -2.7 V_{NHE}.[33]

In Fig. 10 are presented some values from the literature concerning redox potentials of radicals and gold ions, together with potentials of other transient gold states tentatively derived from the reactivities observed in this work. The three-electron redox potential of $Au^{III}Cl_4^-$ reduction into Au^0 on a metal electrode is known to be $E^{\circ}(Au^{III}Cl_4^-/Au_{met}) = 1.002$ V_{NHE}.[34] According to the spontaneous successive disproportionations of Au^{II} into Au^{III} and Au^{I}, and of Au^{I} into Au^{II} and Au^0, the potentials $E^{\circ}(Au^{III}Cl_4^-/Au^{II}Cl_4^{2-})$, $E^{\circ}(Au^{II}Cl_4^{2-}/Au^{I}Cl_2^-)$ and $E^{\circ}(Au^{I}Cl_2^-/Au_{met}, Cl^-)$ should increase in this order. We assigned the delay before the observation of any absorbance at 520 nm at low dose (Fig. 2) to a stabilization of Au^{I} with respect to the disproportionation because this process is thermodynamically unfavored when Au^{I} is free [eqn. (15)]. Actually, the corresponding potential

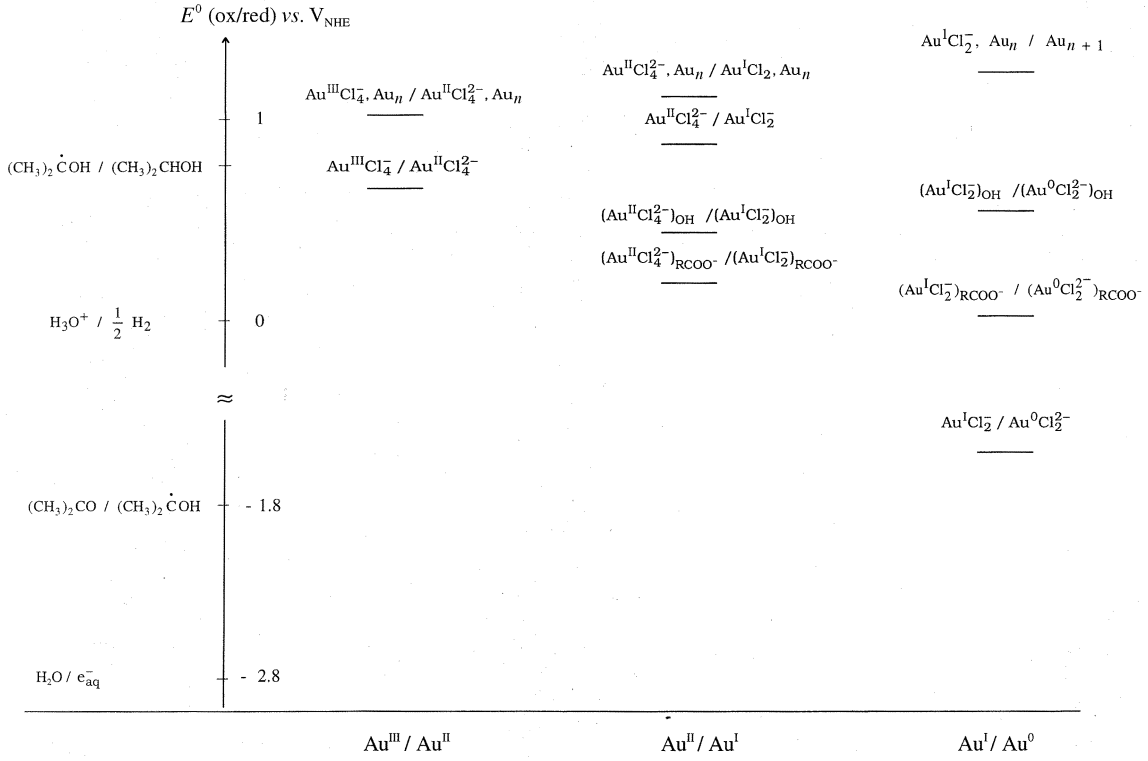

Fig. 10 Scheme of the redox potentials of gold ions of intermediate valencies compared to the potentials of some reducing radicals.[14,15,17,34] Some potential values are tentatively proposed according to the experimental observations (see text)

$E^\circ(Au^I/Au^0)$ is rather low, probably in the same range as for the cyanide complex (-1.5 V_{NHE}).[12] In contrast, the disproportionation [reaction (11)] occurs readily if the solution already contains clusters (formed during the irradiation or added) because they behave as small electrodes and the condition of eqn. (14) is fulfilled. The reaction rate of Au_n formation increases with Au_n concentration (or OD_{520}) as in a catalytic process.

The reaction is also favored by the presence of alcohol groups, and more so by 2-propanol than by PVA. In fact, in 2-propanol solutions the process is achieved within the irradiation time and at the end of irradiation the reduction of Au^I and the formation of Au^0 is complete with a value of $G(\text{red}) = 6$ (Fig. 5). That means that the overall reduction of Au^{III} is at this moment exclusively due to the radiolytic species.

An important change of the Au^I lifetime results from the presence of PVA, as shown by comparison of the curves of Fig. 5 and Figs. 6 and 7. However, the induction time, which depends on the disproportionation of Au^I, does decrease as the PVA concentration increases. The PVA alcohol groups are less active than those of 2-propanol, possibly because of an inhibiting role of the carboxylate groups coexisting with the alcohol functions in PVA.

Complexation equilibria control the interactions of the gold ions or clusters with the main ligand Cl^- and also with the carboxylate or the alcohol groups of PVA and 2-propanol. These types of interactions are known to influence the redox potentials of the couples. Therefore, the fate of Au^I is strongly dependent on the extent of the complexation with alcohol, which was already invoked:[8]

$$Au^ICl_2^- + PVA(OH) \rightarrow (Au^ICl_2^-)_{PVA(OH)} \quad (17)$$

$$Au^ICl_2^- + ROH \rightarrow (Au^ICl_2^-)_{ROH} \quad (18)$$

Similarly, Au^{II} and Au^0 may also be complexed.

The relative potential values of the couples Au^{II}/Au^I and Au^I/Au^0, in which Au^I is involved, govern the occurrence and the rate of the disproportionation. In the absence of alcohol and at low dose, when no cluster is yet formed, the $Au^ICl_2^-$ disproportionation is not favored because the redox potential between Au^I ions and single atoms $E^\circ(Au^I/Au^0)$ is negative so that $E^\circ(Au^I/Au^0) < E^\circ(Au^{II}/Au^I)$ [eqn. (15) Fig. 10]. In the presence of 2-propanol, on the contrary, it seems that the disproportionation is allowed as if now $E^\circ(Au^I_{ROH}/Au^0_{ROH}) > E^\circ(Au^{II}_{ROH}/Au^I_{ROH}) > E^\circ(O_2/O_2^-) = -0.33$ V_{NHE}. Therefore, reaction (19) is fast and no induction time is observed:

$$2(Au^ICl_2^-)_{ROH} \rightarrow (Au^0Cl_2^{2-})_{ROH} + (Au^{II}Cl_2)_{ROH} \quad (19)$$

It is followed by reaction (6), so that the overall reduction reaction is:

$$3(Au^ICl_2^-)_{ROH} \rightarrow 2(Au^0Cl_2^{2-})_{ROH} + (Au^{III}Cl_4^-)_{ROH} \quad (20)$$

According to these observations, the potentials with ROH must be in the order $E^\circ(Au^{III}/Au^{II}) < E^\circ(Au^{II}/Au^I) < E^\circ(Au^I/Au^0)$, as tentatively proposed in Fig. 10

To a lesser extent, the alcohol groups of PVA may play the same role but their interaction with gold is partly inhibited by the carboxylate bonds. The induction time is just shortened by increasing the PVA concentration (Fig. 5 and 6). At the highest PVA concentrations, the disproportionation may occur within the irradiation period and after the end of irradiation the kinetics of step I are accelerated by the presence of PVA (Fig. 5 and 6). The results suggest that complex species are formed with the carboxylate groups in competition with reaction (17):

$$Au^ICl_2^- + PVA(COO^-) \rightarrow (Au^ICl_2^-)_{PVA(COO^-)} \quad (21)$$

These Au^I ions complexed by $PVA(COO^-)$ do not disproportionate, in contrast with reaction (19). Thus, the redox potentials are now such that

$$E^\circ(Au^I/Au^0)_{PVA(COO^-)} < E^\circ(Au^{II}/Au^I)_{PVA(COO^-)} \quad (22)$$

At long times after the end of irradiation, when clusters have been slowly formed and the adsorption of Au^I on them is favored, reaction (11) is allowed. As for Au^{III}, the reduction of adsorbed Au^I by an alcohol group becomes also possible.

The scheme in Fig. 10 tentatively summarizes the relative values of the potentials, accounting for the processes observed. The order of eqns (13) and (14) explains the catalysis by Au_n. In addition, the potential order of complexed Au^I ions explains how the stability of Au^I, particularly with respect to its disproportionation, depends on the complexation conditions. The redox potential of 2-propanol must be higher than that of the couple of free Au^{III}/Au^{II} but slightly lower than that of the ions adsorbed on a particle [eqn. (13)].

Cluster growth

As shown by the AFM observations, the final size of the gold clusters depends markedly on the conditions of the reduction of the ionic precursors. The detailed study of the process kinetics allows us to propose a mechanism that explains how the final size is controlled and which parameters are decisive. At first, the process in the bulk must be initiated by the reduction of Au^{III}, which requires a reducing agent with a redox potential at least lower than $E^\circ(Au^{III}/Au^{II})$. Then Au^{II} disproportionation occurs readily. The next step from Au^I to Au^0 is crucial for cluster growth. In fact, three scenarios are possible.

(*i*) The potential of the reducing agent is quite negative relative to $E^\circ(Au^I/Au^0)$. Solvated electrons (or alcohol radicals) produced by irradiation (ionizing radiation or photons) fulfill this condition and totally reduce the ions to zerovalent gold. Moreover, if the amount of reducing equivalents is provided to the gold solution fast enough, as in the high dose rate experiments, the intermediate valency Au^I is also immediately reduced, so that the preferential reduction of Au^{III} and the stabilization of Au^I are avoided. Eventually the gold atoms yielded separately by the reduction coalesce according to a homogeneous nucleation controlled by the surfactant, explaining that the sizes are the smallest observed.

(*ii*) If Au^I is formed by a partial radiolytic reduction but not reduced by a chemical agent [whose redox potential is too positive relative to $E^\circ(Au^I/Au^0)$, which is the most common situation for molecules in the absence of solid nuclei], Au^I disproportionates very slowly (faster if complexed by alcohols, for example) and as soon as formed the few clusters catalyze the disproportionation. Then, the surfactant does not inhibit the adsorption of ions on the same clusters or the electron transfer from the chemical agent to the ions adsorbed. Therefore, the growth process depends, as in a photographic development, on the concentration of clusters, on the total concentration of ions to be reduced and on the redox potential of the reducing agent. The final cluster size is much higher than in (*i*).

(*iii*) Without initial irradiation for even partial reduction, the Au^I ions, formed by chemical reduction of Au^{III} and disproportionation of Au^{II}, accumulate and the Au^I disproportionation is greatly delayed because, unless they are adsorbed on clusters or complexed by special ligands, the potentials are not suitable. The number of clusters so formed being quite scarce, the catalysis of the disproportionation is restricted to extremely diluted nucleation centers and each of these nuclei develops and grows dramatically.

Conclusions

The radiolytic reduction of auric ions let appear critical conditions to form the zerovalent species: the low valency Au^I ions are somewhat protected by the more concentrated Au^{III} ions

from reduction. In the presence of alcohol functions, the complexed Au^{I} ions disproportionate while ions interacting with carboxylate do not. The clusters yielded by the coalescence of the atoms formed catalyze also the disproportionation reaction. At longer times, Au^{III} or Au^{I} adsorbed on clusters resulting from the radiolysis are reduced by alcohol molecules and contribute to develop the nuclearity of these same clusters by acting as growth nuclei. As shown by micrographs, under these conditions the gold atoms are eventually distributed into particles containing at least 10^3 more atoms each than when the reduction is achieved completely by irradiation. The difference arises from the occurrence in the radiolysis of independant Au^{III} reduction processes by strongly reducing radicals, which react at each encounter. Provided that the disproportionation of Au^{I} may be accelerated without the need for catalysis by early clusters, isolated atoms formed by this disproportionation coalesce under control of the surfactant. In contrast, chemical reduction of Au^{III}, by an alcohol for example, which is a weak reducing agent and as such constitutes an extreme case, requires preformed clusters as catalysts and therefore results essentially in their development up to large clusters.

Note that the adsorption of Au^{I} on various supports or its complexation could also favor the disproportionation, which governs the whole reduction process. These steps must certainly be taken into account in the explanation of geological processes of speciation and precipitation of gold.

More generally, the analysis of the elementary steps of the reduction, radiolytic or chemical, of multivalent ions whose behavior for the last reduction step $M^{I} \rightarrow M^{0}$ should be comparable to $Au^{I} \rightarrow Au^{0}$, enables us to understand better the factors governing the final size of the clusters and thus to use this information in order to control their synthesis.

References

1 J. Belloni, J. Amblard, J. L. Marignier and M. Mostafavi, *Clusters of Atoms and Molecules*, ed. H. Haberland, Springer-Verlag, Berlin, 1994, vol. II, pp. 290–311.
2 A. Henglein, *Chem. Rev.*, 1989, **89**, 1861.
3 J. S. Bradley, *Clusters and Colloids*, ed. G. Schmid, Weinheim, New York, 1994, pp. 459–544.
4 A. Henglein, *Ber. Bunsenges. Phys. Chem.*, 1995, **99**, 903.
5 J. Belloni, *Curr. Op. Colloid Interface Sci.*, 1996, **1**, 184.
6 A. Henglein, *J. Phys. Chem.*, 1993, **97**, 5457.
7 G. V. Buxton and R. M. Sellers, *Coord. Chem. Rev.*, 1977, **22**, 195.
8 M. Quinn and G. Mills, *J. Phys. Chem.*, 1994, **98**, 9840.
9 L. Longenberger and G. Mills, *J. Phys. Chem.*, 1995, **99**, 475.
10 B. G. Ershov and N. L. Sukhov, *Radiat. Phys. Chem.*, 1990, **36**, 93.
11 B. G. Ershov, N. L. Sukhov and D. I. Troitskii, *Radiat. Phys. Chem.*, 1992, **39**, 127.
12 S. Mosseri, A. Henglein and E. Janata, *J. Phys. Chem.*, 1989, **93**, 6791.
13 D. G. Duff, A. Baiker and P. P. Edwards, *Langmuir*, 1993, **9**, 2310.
14 A. J. Swallow, *Radiation Chemistry: An Introduction*, Wiley, New York, 1973.
15 H. A. Schwarz, *J. Chem. Educ.*, 1981, **59**, 101.
16 A. S. Gosh-Mazumdar and E. J. Hart, *Adv. Chem. Ser.*, 1968, **81**, 193.
17 H. A. Schwarz and R. W. Dodson, *J. Phys. Chem.*, 1989, **93**, 409.
18 J. H. Baxendale and A. M. Koulkes-Pujo, *J. Chim. Phys.*, 1970, **67**, 1602.
19 J. L. Marignier, Thèse d'Etat, Université Paris XI, Orsay, 1987.
20 J. J. Lingane, *J. Electroanal. Chem.*, 1962, **4**, 332.
21 C. H. Gammons, Y. Yu and A. E. Williams-Jones, *Geochim. Cosmochim. Acta*, 1997, **61**, 1971.
22 A. M. Koulkes-Pujo and S. Rashkov, *J. Chim. Phys.*, 1967, **64**, 534; *ibid.*, 1968, **65**, 911.
23 G. Mills and A. Henglein, *Radiat. Phys. Chem.*, 1985, **26**, 391.
24 N. Kegouche, Thèse 3ème cycle, Université Paris XI, Orsay, 1983.
25 M. Michaelis and A. Henglein, *J. Phys. Chem.*, 1992, **96**, 4719.
26 J. Khatouri, M. Mostafavi, J. Amblard and J. Belloni, *Chem. Phys. Lett.*, 1992, **191**, 351; J. Khatouri, M. Mostafavi, J. Ridard, J. Amblard and J. Belloni, *Z. Phys. D: Atoms Mol. Clusters*, 1995, **34**, 57.
27 B. G. Ershov, E. Janata and A. Henglein, *Radiat. Phys. Chem.*, 1992, **39**, 123; B. G. Ershov, *Russ. Chem. Bull.*, 1994, **43**, 16.
28 J. L. Marignier and J. Belloni, *J. Chim. Phys.*, 1988, **85**, 21.
29 B. Keita, L. Nadjo, E. Gachard, H. Remita, J. Khatouri and J. Belloni, *New J. Chem.*, 1997, **21**, 851.
30 M. Mostafavi, J. L. Marignier, J. Amblard and J. Belloni, *Radiat. Phys. Chem.*, 1989, **34**, 605; *Z. Phys. D: Atoms Mol. Clusters*, 1989, **12**, 31.
31 Z. Y. Huang, G. Mills and B. Hajek, *J. Phys. Chem.*, 1993, **97**, 11542.
32 S. Remita, P. Archirel and M. Mostafavi, *J. Phys. Chem.*, 1995, **99**, 12198.
33 J. H. Baxendale and R. S. Dixon, *Z. Phys. Chem.*, 1964, **43**, 161.
34 *Handbook of Chemistry and Physics*, ed. D. R. Lide, CRC Press, Boston, 72nd edn., 1991.

Received in Montpellier, France, 11th June 1998;
Paper 8/04445G